Available online at www.sciencedirect.com
ScienceDirect
Journal of Solid State Chemistry 179 (2006) 3672–3680
JOURNAL OF SOLID STATE CHEMISTRY
www.elsevier.com/locate/jssc

Synthesis, crystal structure and magnetic properties of new indium rhenium and scandium rhenium oxides, In_6ReO_{12} and Sc_6ReO_{12}

D. Mikhailova*, H. Ehrenberg, H. Fuess

Institute for Materials Science, Darmstadt University for Technology, Petersenstr. 23, D-64287, Darmstadt, Germany

Received 11 May 2006; received in revised form 25 July 2006; accepted 29 July 2006
Available online 4 August 2006

Abstract

The new complex indium rhenium and scandium rhenium oxides, In_6ReO_{12} and Sc_6ReO_{12}, have been synthesized as single phases in sealed silica tubes and by high-pressure high-temperature syntheses, and their crystal structures have been determined by single crystal X-ray diffraction.The compounds crystallize in a rhombohedral structure related to the distorted fluorite structure like Ln_6ReO_{12} for some rare earth elements, S. G.: *R*-3, $Z = 3$, $a_H = 9.248(2)$ Å, $c_H = 8.720(2)$ Å for Sc_6ReO_{12} and $a_H = 9.492(1)$ Å, $c_H = 8.933(1)$ Å for In_6ReO_{12}. A maximum in magnetization is observed for Sc_6ReO_{12} at $T(M_{max}) = 1.89(2)$ K, whereas ferromagnetic ordering is found for In_6ReO_{12} by a pronounced increase in the temperature dependence of magnetization at $T_C = 7.5(5)$ K. The magnetic moment per rhenium ion in In_6ReO_{12} and Sc_6ReO_{12} is 0.84(1) and 0.65(1) μ_B, respectively, derived from the paramagnetic regions.

PACS: 61.66.Fn

Keywords: Indium rhenium oxide In_6ReO_{12}; Scandium rhenium oxide Sc_6ReO_{12}; Distorted fluorite structure; Magnetism of Re^{+6}

1. Introduction

Ln_6MeO_{12} compounds, crystallizing in space group *R*-3 with a distorted fluorite-type structure, are known in the MeO_3–Ln_2O_3 system, where *Me*–Mo, W, Re or *U*, and *Ln*–some rare earth elements [1–3]. The same structure is adopted by some ordered Ln_7O_{12} phases (*Ln* = Ce, Pr, Tb) [2]. These authors have proposed a critical ratio between the ionic radii of the hexavalent metal ions and the trivalent rare earth ion to be equal about 0.67 or more as an empirical criterion for the formation of the Ln_6MeO_{12} phases with a rhombohedral structure for *Me* = Mo, W, U. But some Ln_6ReO_{12} phases with this rhombohedral structure exist [3], where the ionic radii ratio Re^{+6}/Ln^{3+} is smaller than for the molybdates, tungstates and uranates, for example, Ho_6ReO_{12} with $r(Re^{+6})/r(Ho^{+3}) = 0.61$ [4]. In a previous work [3] the synthesis and investigation of magnetism of Ln_6ReO_{12} compounds (*Ln* = Ho, Er, Tm, Yb and Lu) were presented. Rhenates of rare earth elements show different magnetic properties depending on the rare earth ion, a magnetic moment of 0.74 μ_B per Re^{+6} was deduced for Lu_6ReO_{12} (Lu^{3+} itself is diamagnetic).

Sc- and In-containing rhombohedral phases Sc_6MoO_{12}, Sc_6WO_{12} [5,6] and In_6WO_{12} [7,8] are also known. The Sc^{3+} and In^{3+} ions resemble heavy rare earth ions in different compounds despite of their smaller ionic radii [9]. In the systems Sc–Re–O and In–Re–O only perrhenates $Sc(ReO_4)_3$ and $In(ReO_4)_3$ are known [5,10,11], and the crystal structure of $Sc(ReO_4)_3 \cdot 3H_2O$ [12] and In $(ReO_4)_3 \cdot 4.5H_20$ [13] were determined. In this work we report the synthesis of Sc_6ReO_{12} by two different methods, in a sealed silica tube and by a high pressure high temperature (HPHT) method, the synthesis of In_6ReO_{12} by a high-pressure high-temperature method, the structure determination by single-crystal X-ray diffraction, and an investigation of magnetic properties of these compounds.

*Corresponding author. Fax: +49 6151 166023.
E-mail address: mikhailova@st.tu-darmstadt.de (D. Mikhailova).

0022-4596/$ - see front matter © 2006 Elsevier Inc. All rights reserved.
doi:10.1016/j.jssc.2006.07.041

2. Experimental

One- and two-temperature syntheses in sealed silica tubes. Samples of nominal composition Sc_6ReO_{12} were synthesized in sealed silica tubes using Sc_2O_3 (Strem Chemicals, 99.99%) and ReO_3 (Strem Chemicals, 99.9%) or Re (Alfa Aesar, 99.997%) and Re_2O_7 (Alfa Aesar, 99.9%) as starting materials. A stoichiometric mixture of Sc_2O_3 and ReO_3 was ground in an agate mortar under acetone and pressed into pellets, which were placed in an Al_2O_3 crucible, sealed in an evacuated silica tube (ordinary optical grad, water content 30 ppm), and annealed in a muffle furnace. In a two-temperature synthesis two pellets of Sc_2O_3 and ReO_3 mixture in two crucibles were divided from each other by a small quartz stick and placed in a silica tube. The tube was evacuated and placed into a tube furnace with a temperature gradient. Before use, Sc_2O_3 and ReO_3 were dried in air at 110–115 °C for 2–3 h, silica tubes and Al_2O_3 crucibles were dried in the oxypropane flame. If Re and Re_2O_7 were used as Re source, a powder mixture of Re, Sc_2O_3 and Re_2O_7 oxides in the molar ratio 1:21:3 was placed within a glove box into a silica tube using an Al_2O_3 crucible. The tube was sealed under vacuum.

High-pressure high-temperature synthesis: A high-pressure synthesis of In_6ReO_{12} and Sc_6ReO_{12} was performed in a Girdle-Belt apparatus with pyrophyllite as the pressure-transmitting medium. A graphite furnace and a platinum capsule containing the reactants were used for the experiment. A mixture of In_2O_3 (Alfa Aesar, 99.99%) and ReO_3 (Strem Chemicals, 99.9%) in molar ratio In:Re = 6:1 or a mixture of one mole of Sc_2O_3, one mole of ReO_2 (Alfa Aesar, 99.9%) and one mole of ReO_3 with nominal composition "$ScReO_4$" was ground in an agate mortar under acetone and filled in a platinum capsule. The sample holder was pressed up to 50 kbar before the temperature was raised to 1300 °C with a rate of 50°/min. The heating current was switched off after 120 min and after cooling to room temperature, pressure was released.

Single-crystal X-ray *diffraction*: The crystal structure of In_6ReO_{12} and Sc_6ReO_{12} was solved by single-crystal X-ray diffraction using the Xcalibur system from Oxford Diffraction. The software packages SHELXS [14] and SHELXL [15] were used for structure solution and refinement as included in X-STEP32 [16]. A combined empirical absorption correction with frame scaling was applied, using the scale3 abspack command in CrysalisRed [17].

X-ray *powder diffraction (XPD)*. Phase analysis and determination of cell parameters were carried out using X-ray powder diffraction with a STOE STADI P diffractometer (Mo-$K\alpha_1$-radiation, $\lambda = 0.7093$ Å) in steps of 0.02° for 2Θ from 3 to 45° in transmission mode. All diffraction patterns have been analyzed by full-profile Rietveld refinements, using the software package WinPLOTR [18].

Thermogravimetry (TG). The Re content in the Sc_6ReO_{12} samples was determined by thermogravimetric

Table 1
Conditions and results of (a)one-temperature syntheses and (b) two-temperature synthesis of Sc_6ReO_{12}

No.	Starting materials	T (°C)	Time (h)	Products (wt%)	Cell parameters of Sc_6ReO_{12} (Å)
(a)					
1	$Sc_2O_3 + ReO_3$ ("Sc_6ReO_{12}")	950	18	Sc_2O_3–90%, 10%–unknown phase	
2	$Re + Sc_2O_3 + Re_2O_7$ ("Sc_6ReO_{12}")	1000	41	Sc_6ReO_{12}–43% Sc_2O_3–52%, 5%–unknown phase	$a = 9.2463(2)$, $c = 8.7119(2)$
3	$Sc_2O_3 + ReO_3$ ("Sc_6ReO_{12}")	1010	33	Sc_6ReO_{12}–50% Sc_2O_3–46% ReO_2–4%	$a = 9.2444(3)$, $c = 8.7126(3)$
4	$Sc_2O_3 + ReO_3$ ("Sc_6ReO_{12}")	1050	16	Sc_6ReO_{12}–57% Sc_2O_3–37%, ReO_2–6%	$a = 9.2450(2)$, $c = 8.7123(3)$
5	$Sc_2O_3 + ReO_3$ ("Sc_6ReO_{12}")	1080	50	Sc_6ReO_{12}–7% Sc_2O_3–85%, ReO_2–6% 2%–unknown phase	$a = 9.251(1)$, $c = 8.718(1)$
(b)					
1	$Sc_2O_3 + ReO_3$ ("Sc_6ReO_{12}") $Sc_2O_3 + ReO_3$ ("Sc_6ReO_{12}")	$T_2 = 1010$ $T_1 = 1020$	33	Sc_6ReO_{12}–100% Sc_6ReO_{12}–91% Sc_2O_3–9%	$a = 9.2451(2)$, $c = 8.7148(2)$ $a = 9.2455(1)$, $c = 8.7141(2)$Å
2	$Sc_2O_3 + ReO_3$ ("Sc_6ReO_{12}") $Sc_2O_3 + ReO_3$ ("Sc_6ReO_{12}")	$T_2 = 1025$ $T_1 = 1035$	91	Sc_6ReO_{12}–72% Sc_2O_3–28% Sc_6ReO_{12}–50% Sc_2O_3–45% +5% unknown phase	$a = 9.2478(1)$, $c = 8.7178(2)$ $a = 9.2479(3)$, $c = 8.7168(4)$

measurements. The method is based on the ability of Re in a number of complex oxides to be oxidized to volatile Re_2O_7 by heating in air. Samples were carefully weighed in Al_2O_3 crucibles before and after annealing in air at 950 °C during 24 h. The Re content in the samples was estimated assuming that the mass loss corresponds to ReO_3 oxide. The phase composition of the residue (Sc_2O_3) was always checked by X-ray diffraction.

Magnetic susceptibility. The magnetic properties of In_6ReO_{12} and Sc_6ReO_{12} have been studied with a superconducting quantum interference device (SQUID) from Quantum Design. Measurements were performed upon heating in the temperature range from 1.7 to 300 K and with an applied field strength of 500 G, both in field-cooled (FC) and zero-field cooled (ZFC) mode.

3. Results and discussion

3.1. Synthesis and characterization of Sc_6ReO_{12} samples

3.1.1. One- and two-temperature synthesis in a sealed silica tube

Conditions and results of one-temperature Sc_6ReO_{12} synthesis in a sealed silica tube are presented in Table 1(a). The amount of Sc_6ReO_{12} phase in the products changes with increasing synthesis temperature from 950 to 1080 °C. No Sc_6ReO_{12} was found in reaction products after synthesis at 950 °C, and the maximal Sc_6ReO_{12} content was found after synthesis at 1050 °C. Sc_2O_3 and ReO_2 were always detected as admixtures in the syntheses. This can be explained by taking into account some reaction, which takes place in the silica tube at high temperatures. Rhenium(VI) oxide ReO_3 is not stable under heating and decomposes at 630 °C into ReO_2 and Re_2O_7 [19] according to

$$3ReO_3(s) \Rightarrow ReO_2(s) + Re_2O_7(g). \quad (1)$$

The reaction with Sc_2O_3 occurs partly through the gas phase:

$$9Sc_2O_3(s) + ReO_2(s) + Re_2O_7(g) \Leftrightarrow 3Sc_6ReO_{12}(s). \quad (2)$$

The estimated value of Re_2O_7 pressure inside the silica tube during the synthesis at 1050 °C was about 0.3 atm. For this estimation a pellet of the reacting mixture was weighed before the synthesis and after quenching the tube into water from synthesis temperature. It is assumed that the mass difference of the pellet corresponds to Re_2O_7 evaporation.

In order to facilitate the formation of the Sc_6ReO_{12} phase according to reaction (2), the Re_2O_7 partial pressure must be higher than the equilibrium value [20]. We have performed some experiments with a fixed Re_2O_7 pressure in a reaction tube applying two-temperature synthesis as described in [21,22], in which complex oxides containing Hg had been prepared. At higher temperature T_1 a mixture of Sc_6ReO_{12}, Sc_2O_3 and ReO_2 was used to adjust the Re_2O_7 partial pressure in the tube, whereas in the lower-temperature region single phase Sc_6ReO_{12} must be formed, because the Re_2O_7 pressure in the tube is higher than the one at $T_2 < T_1$. The use of the two-temperature method in a sealed tube gives good results if the synthesis time is about 30–40 h (experiment 1, Table 1b and Fig. 1(a)). If the synthesis was performed during 90 h or more, the Sc_6ReO_{12} amount in the products reduced to 70% and Sc_2O_3 was found as an impurity (experiment 2, Table 1b). In this case a lot of small black shining ReO_2 crystals were found on the walls of the coldest part of the tube. It is known that in the system Re–O at 800–1000 °C ReO_2 crystals can be easily grown during some days by means of chemical transport reactions with water molecules as a transport agent [23]. The author of [23] noted, that water traces in an ordinary silica glass are enough for the ReO_2 transport. Therefore, due to Re transport in form of ReO_2, its content in samples decreases and Sc_2O_3 appears as a second phase. The synthesis time must be reduced to 20–30 h in order to avoid loss of ReO_2.

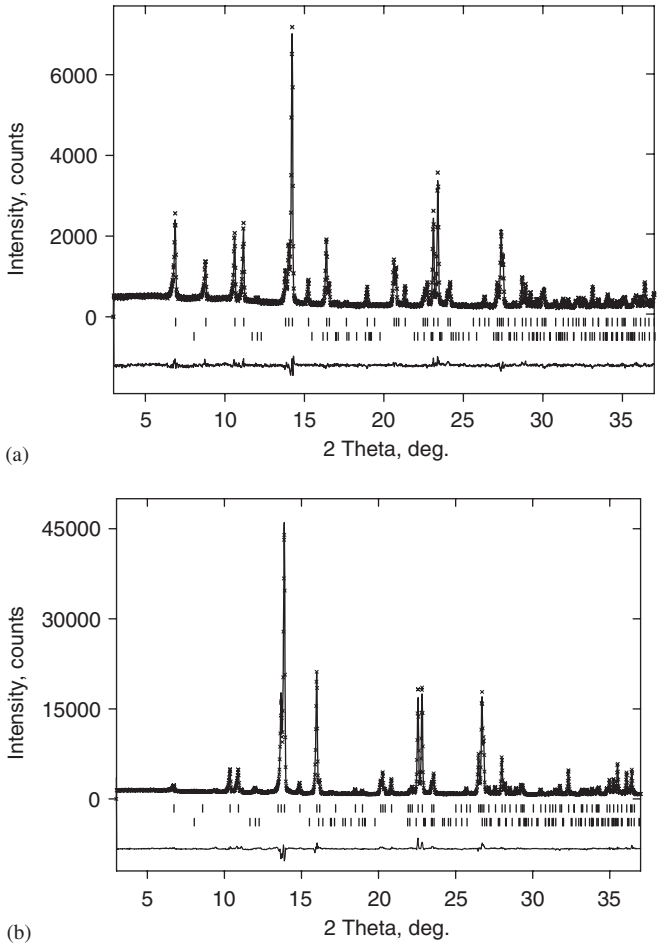

Fig. 1. The observed and fitted profiles together with the corresponding difference curve (Mo-$K\alpha_1$): (a) for Sc_6ReO_{12} obtained by two-temperature synthesis and (b) for In_6ReO_{12} obtained by high-pressure high-temperature synthesis. The reflection marks at the bottom belong to the monoclinic phase ReO_2, 0.5 wt% and 1.5 wt% in Sc_6ReO_{12} and In_6ReO_{12} samples, respectively.

Note that the syntheses of Ln_6ReO_{12} (Ln = Ho, Er, Tm, Yb and Lu) phases at 1200 °C in Pt/Rh-tubes were always accompanied by forming of Ln_3ReO_8 as impurity and never ReO_2, which could be due to thermal decomposition of ReO_2 [19] according to

$$7ReO_2(s) = 3Re(s) + 2Re_2O_7(g). \quad (3)$$

and the stability of Ln_3ReO_8 phases in the system Ln_2O_3–Re_2O_7 [24,25] at this temperature. Scandium perrhenate $Sc(ReO_4)_3$ is not stable above 735 °C and decomposes to Re_2O_7(g) and Sc_2O_3. The compound Sc_3ReO_8 is not known [5].

In all samples the Sc_6ReO_{12} phase appears as small dark grey crystals with a size up to 0.05–0.1 mm. The compound is stable in air at least for 1 month. The diffractogram of single phase Sc_6ReO_{12}, prepared by the two-temperature synthesis, is presented in Fig. 1(a). All reflections were explained based on a rombohedral unit cell with lattice parameters $a = 9.25$ Å and $c = 8.72$ Å. According to the thermogravimetric measurements the sample contains 63.7 wt% Sc_2O_3, which corresponds to the chemical composition Sc_6ReO_{12}.

3.1.2. High-pressure high-temperature synthesis

The formation of Sc_6ReO_{12} crystals is also observed under high pressure up to 50 kbar and temperature up to 1300 °C. According to X-ray diffraction the sample with nominal composition "$Sc_2Re_2O_8$" contained after synthesis 49 wt% Sc_6ReO_{12} and 51 wt% ReO_2. All reflections which do not belong to ReO_2 were explained based on a rhombohedral unit cell with lattice parameters $a = 9.2451(2)$ Å and $c = 8.6988(3)$ Å. Note, that the sample obtained in absence of the gas phase (HPHT synthesis) has a smaller "c" parameter at the same "a" parameter in comparison with the sample prepared in the quartz tube at lower temperature (Table 1b, $a = 9.2451(2)$ Å and $c = 8.7148(2)$ Å).

3.2. Synthesis and characterization of In_6ReO_{12} samples

In_6ReO_{12} was successfully synthesized by high-pressure high-temperature synthesis only, attempts to prepare In_6ReO_{12} samples in a sealed silica tube led to formation of ReO_2 and $In(ReO_4)_3 \cdot 4.5H_2O$ as reaction products according to X-ray diffraction at ambient conditions. The

Table 2
Details of X-ray single-crystal data collection and structure refinement of Sc_6ReO_{12} and In_6ReO_{12}.

Crystal data		
Chemical formula	Sc_6ReO_{12}	In_6ReO_{12}
Formula weight	647.96	1067.12
Crystal system	Rhombohedral	Rhombohedral
Space group	R -3 (no. 148)	R -3 (no. 148)
Unit cell dimensions		
Hexagonal axes	$a_H = 9.248(2)$ Å	$a_H = 9.492(1)$ Å
	$c_H = 8.720(2)$ Å	$c_H = 8.933(1)$ Å
Rhombohedral axes	$a_R = 5.836(3)$ Å	$a_R = 5.985(2)$ Å
	$\alpha = 97.35(1)$ Å	$\alpha = 97.397(6)$ Å
Cell volume	645.87(20) Å^3	697.02(13) Å^3
Z	3	3
Calculated density (g/cm^3)	4.997	7.627
Radiation type	Mo-$K\alpha$, $\lambda = 0.71073$ Å	Mo-$K\alpha$, $\lambda = 0.71073$ Å
No. of reflections for cell parameters	372	1215
Temperature (K)	293(2)	293(2)
Crystal form, colour	Prismatic, black	Prismatic, black
Crystal size (mm^3)	0.050 0.030 0.020	0.050 · 0.045 · 0.045
Data collection		
Diffractometer	Oxford Diffraction Xcalibur; single-crystal X-ray diffractometer with sapphire CCD detector	
Data collection method	Rotation method data acquisition using ω and φ scans(s)	
Absorption coefficient	18.510 mm^{-1}	27.662 mm^{-1}
F(000)	891	1395
Range for data collection	3.45 to 29.78°	3.37 to 36.65°
Range of h, k, l	$-12 \leqslant h \leqslant 12$, $-11 \leqslant k \leqslant 12$, $-11 \leqslant l \leqslant 10$	$-13 \leqslant h \leqslant 13$, $-13 \leqslant k \leqslant 15$, $14 \leqslant l \leqslant 14$
D (min), d (max) for cell determination (Å)	0.737, 5.93	0.60, 6.1
Reflections collected/unique	1007/963	2203/755
Completeness to $\theta = 26.35°$ (36.65°)	0.921	0.975
Refinement method	Full-matrix least-squares on F^2	
Data/restraints/parameters	963/0/31	755/0/31
Goodness-of-fit on F^2	1.106	1.107
Final R indices [$I > 2$sigma(I)]	$R_1 = 0.0530$, w$R_2 = 0.1414$	$R_1 = 0.0224$, w$R_2 = 0.0546$
R indices (all data)	$R_1 = 0.0595$, w$R_2 = 0.1588$	$R_1 = 0.0267$, w$R_2 = 0.0555$
Largest diff. peak and hole	3.16, −2.59 e/Å^3	2.031, −1.622 e/Å^3

presence of water molecules in indium perrhenate must be due to exposure of the sample to air during X-ray diffraction for some hours; it is known that the most of perrhenates of two- and three-valent metals are stable in air only in the form of hydrates [12,13]. The initial compound In_2O_3 was always observed. The diffractogram of In_6ReO_{12} is shown in Fig. 1(b). Almost all reflections were explained based on a rhombohedral unit cell with lattice parameters $a = 9.4658(2)$ Å, $c = 8.9136(2)$ Å (in hexagonal setting), except one peak at $2\theta = 12^{o}$ which belongs to monoclinic ReO_2 (1.5 wt%).

3.3. Structural features of In_6ReO_{12} and Sc_6ReO_{12}

According to X-ray structure analysis of In_6ReO_{12} single crystals and twinned Sc_6ReO_{12} crystals, the compounds crystallize in a distorted anion-deficient fluorite-type structure with formally six oxygen vacancies per one cell on the threefold axes like some Ln_6MO_{12} compounds where Ln is some rare earth element and M = Mo, W, Re or U (space group R-3, $a = 9.492(1)$ Å, $c = 8.933(1)$ Å for In_6ReO_{12} and $a = 9.248(2)$ Å, $c = 8.720(2)$ Å for Sc_6ReO_{12} (Table 2).

In the case of Sc_6ReO_{12} all observed reflections can only be indexed based on a 2-domain crystal. The orientations of the two domains with respect to each other are given by the following relations:

$$a_1^* = -17/21 \cdot a_2^* + 8/21 \cdot b_2^* - 16/21 \cdot c_2^*,$$

$$b_1^* = 5/21 \cdot a_2^* - 11/21 \cdot b_2^* - 20/21 \cdot c_2^*,$$

$$c_1^* = -1/3 \cdot a_2^* - 2/3 \cdot b_2^* + 1/3 \cdot c_2^*$$

or vice versa

$$a_2^* = -17/21 \cdot a_1^* + 8/21 \cdot b_1^* - 16/21 \cdot c_1^*,$$

$$b_2^* = 5/21 \cdot a_1^* - 11/21 \cdot b_1^* - 20/21 \cdot c_1^*,$$

$$c_2^* = -1/3 \cdot a_1^* - 2/3 \cdot b_1^* + 1/3 \cdot c_1^*,$$

This corresponds to a rotation through 175° about an axis parallel to $-0.334a_1$–$0.591b_1 + 0.735c_1$. The indices are related by

$$h_1 = (-17\,h_2 + 5\,k_2 - 7\,l_2)/21,$$

$$k_1 = (8\,h_2 - 11\,k_2 - 14\,l_2)/21,$$

$$l_1 = (-16\,h_2 - 20\,k_2 + 7\,l_2)/21.$$

Some reflections can be measured without overlap from the other domain, some intensities are only observed as the sum of contributions from both domains. Therefore, the sample is a non-merohedral twin. The non-overlapping reflections of one domain were sufficient to solve the structure using SHELXS [14]. For structure refinement all observed reflections from both domains were considered using the HKL 5 format in SHELXL [15], and the additional refined batch scale factor (BASF) yielded a domain ratio of 0.585:0.415.

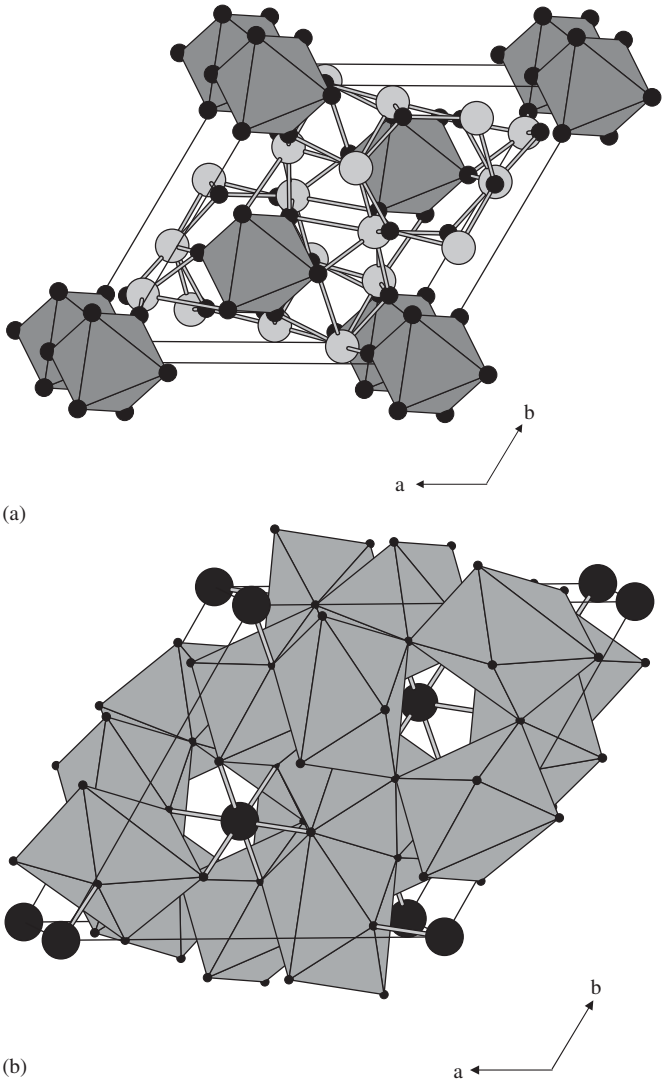

Fig. 2. (a) Separate ReO_6 octahedra in the M_6ReO_{12} (M = In, Sc) cell. Small black spheres are O^{2-} ions, large light grey ones are M^{3+} ions. (b) ScO_7 or InO_7 polyhedra connected via edges and corners. Small black balls are O^{2-} ions, large dark grey ones are Re^{+6} ions.

Table 3
Positional parameters for Sc_6ReO_{12} and In_6ReO_{12}.

Atom	Site	x	y	z	Occup.
Sc_6ReO_{12}					
Re	3a	0	0	0	1
Sc	18*f*	0.2495 (2)	0.0338 (2)	0.3592 (3)	1
O(1)	18*f*	0.1868 (8)	0.0277 (8)	0.1204 (9)	1
O(2)	18*f*	0.2173 (7)	0.0235 (7)	0.6065 (9)	1
In_6ReO_{12}					
Re	3a	0	0	0	1
In	18*f*	0.2496(1)	0.0353(1)	0.3540(1)	1
O(1)	18*f*	0.1822(4)	0.0241(4)	0.1166(4)	1
O(2)	18*f*	0.2195(3)	0.0208(3)	0. 6051(3)	1

Table 4
Anisotropic thermal displacement parameters (Å^2) for Sc_6ReO_{12} and In_6ReO_{12}.

Atom	U_{11}	U_{22}	U_{33}	U_{12}	U_{13}	U_{23}
Sc_6ReO_{12}						
Re	0.0033 (3)	0.0033 (3)	0.0088 (5)	0.00167 (16)	0.00000	0.00000
Sc	0.0046 (8)	0.0054 (8)	0.0083 (9)	0.0033 (6)	−0.0005 (6)	−0.0013 (6)
O(1)	0.008 (3)	0.012 (3)	0.014 (4)	0.004 (2)	−0.004 (3)	−0.002 (3)
O(2)	0.007 (3)	0.003 (2)	0.007 (4)	0.001 (2)	0.007 (3)	0.002 (3)
In_6ReO_{12}						
Re	0.004 (1)	0.004 (1)	0.007 (1)	0.002 (1)	0.000	0.000
In	0.009 (1)	0.008 (1)	0.009 (1)	0.006 (1)	0.000 (1)	−0.001 (1)
O(1)	0.020 (2)	0.020 (2)	0.013 (1)	0.014 (1)	−0.009 (1)	−0.005 (1)
O(2)	0.006 (1)	0.007 (1)	0.008 (1)	0.001 (1)	0.000 (1)	0.000 (1)

Table 5
Selected interatomic distances (Å) for Sc_6ReO_{12} and In_6ReO_{12} compared with some for Sc_6WO_{12} and In_6WO_{12}.

Sc_6ReO_{12}		Sc_6WO_{12} [28]	
Re–O(1)	1.926(6) (× 6)	Re–O(1)	1.90 (× 6)
Sc–O(1)	2.155 (8)	Sc–O(1)	2.20
Sc–O(1)	2.230 (3)	Sc–O(1)	2.20
Sc–O(1)	2.670 (6)		
Sc–O(2)	2.027 (7)	Sc–O(2)	2.00
Sc–O(2)	2.083 (6)	Sc–O(2)	2.10
Sc–O(2)	2.119 (4)	Sc–O(2)	2.10
Sc–O(2)	2.173 (8)	Sc–O(2)	2.20
In_6ReO_{12}		In_6WO_{12} [7]	
Re–O(1)	1.932 (3) (× 6)	W–O(1)	1.93 (× 6)
In–O(1)	2.203 (4)	In–O(1)	2.21
In–O(1)	2.298 (1)	In–O(1)	2.28
In–O(1)	2.727 (3)	In–O(1)	2.77
In–O(2)	2.066 (3)	In–O(2)	2.07
In–O(2)	2.112 (2)	In–O(2)	2.12
In–O(2)	2.227 (1)	In–O(2)	2.21
In–O(2)	2.257 (3)	In–O(2)	2.24

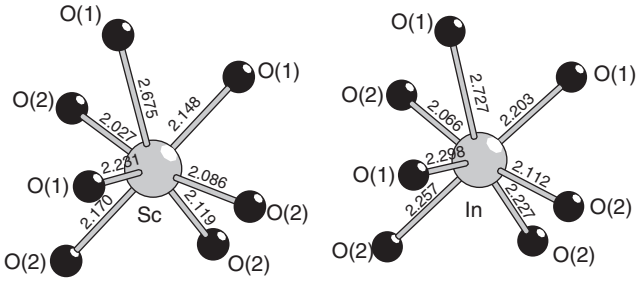

Fig. 3. MO_7-coordination polyhedron (M = Sc, In).

The structure of Sc_6ReO_{12} and In_6ReO_{12} represents a three-dimensional framework formed by octahedra of ReO_6 and monocapped MO_7-prisms (M = In, Sc) connected via edges and corners (Fig. 2a and b). Positional parameters, anisotropic thermal displacement parameters and selected interatomic distances for Sc_6ReO_{12} and In_6ReO_{12} compared with some data for Sc_6WO_{12} and In_6WO_{12} are listed in Tables 3–5, respectively. The interatomic distances in In_6WO_{12} and In_6ReO_{12} or Sc_6WO_{12} and Sc_6ReO_{12} are very similar due to close ionic radii of W^{+6} (0.60 Å) and Re^{+6} (0.55 Å) [4].

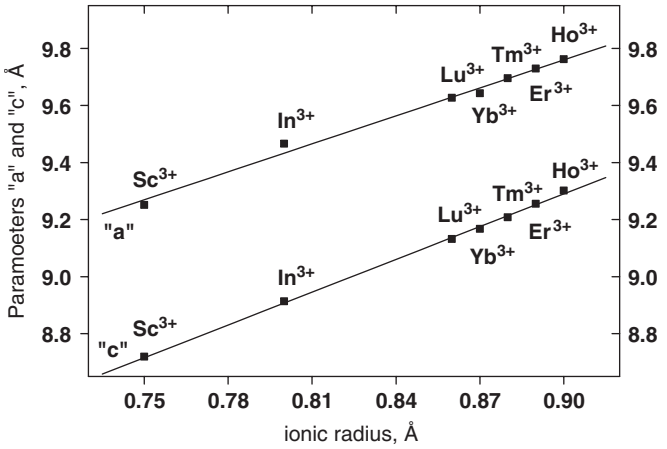

Fig. 4. Dependence of the "a" and "c" cell parameters on the ionic radius [4] of the trivalent cation for Ln_6ReO_{12} (Ln = Ho, Er, Tm, Yb, Lu) [3] and In_6ReO_{12} and Sc_6ReO_{12} (this work).

ReO_6-octahedra are undistorted and isolated from each other, the Re–O interatomic distance d_{Re-O} = 1.926 Å for Sc_6ReO_{12} and 1.932 Å for In_6ReO_{12} is in good agreement with Re–O bond distances observed for other Re containing oxides with a formal rhenium oxidation state of +6: d_{Re-O} = 1.935 Å in $MnReO_4$ [26] or d_{Re-O} = 1.933 Å in Tm_6ReO_{12} [3]. Six Sc–O and In–O bond lengths in the MO_7-polyhedra (Fig. 3) forming a prism lie in an interval of 2.027–2.230 Å for Sc and 2.066–2.298 Å for In, which agrees with average Sc–O and In–O distances in Sc- and In-containing oxides: d_{Sc-O} = 2.12 Å for ScO_6-octahedra in Sc_2O_3 [27] or d_{Sc-O} = 2.13 Å for ScO_6 in Sc_6WO_{12} [28] and d_{In-O} = 2.191 Å for InO_6-octahedra in In_2O_3 [29] or d_{In-O} = 2.27 Å for InO_7 in In_6WO_{12} [7,8]. One M–O distance in MO_7 (2.675 Å for M = Sc and 2.727 Å for M = In) seems to be too long for a regular Sc–O and In–O chemical bond. Nevertheless, we included this oxygen in the coordination sphere of M due to three reasons:

1. The M_6ReO_{12} (M = Sc, In) structure is very close to Ln_7O_{12} (Ln = Tb, Pr, Ce) [2] and Ln_6ReO_{12} (Ln = Ho–Lu) [3]. A dependence of "a" and "c" cell parameters on the ionic radius for Ln_6ReO_{12}, Sc_6ReO_{12} and In_6ReO_{12} (Fig. 4) represents a straight line, demonstrating that all these compounds belong to the same structure type. In these compounds the Ln^{3+} ions have a capped prismatic coordination of 7 oxygen atoms with the usual Ln–O distance [3].
   A model of "coordination defect" has been applied to discuss the Tb_7O_{12} structure [30]. This model considers an oxygen vacancy and six nearest neighbouring oxygen atoms as one structural unit in the close oxygen packing and is based on the defect and relaxation of the anion lattice. It is suggested that oxygen atoms in this structural unit move from ideal fluorite position toward the vacancy due to strong polarization. At the same time the repulsion between the oxygen vacancy and the metal ion has an opposite effect. In MO_7-polyhedra in M_6ReO_{12} (M = Sc, In, Ho–Lu) five O atoms are subjected to the strongest influence of the oxygen vacancy whereas two O atoms with the longest M–O distance remain unaffected. In the case of In_6ReO_{12} and first of all Sc_6ReO_{12} the repulsion between oxygen vacancy and M^{3+} ion is less in comparison with heavy 4f-ions Ln = Ho–Lu, which leads to the more irregular MO_7-polyhedra.
2. The calculations based on the bond-valence model [31–33] with the bond-valence parameters for Sc–O $R_o = 1.849$ and $B = 0.37$ and for In-O $R_o = 1.902$ and $B = 0.37$ [31] gave an oxidation number for Sc of +2.842 and of +2.793 for In in an octahedral coordination, and +2.951 (Sc) and +2.901 (In) for the monocapped prismatic coordination. The latter values are more adequate for the chemistry of these metals.
3. There are more examples with long distances M–O (M = Sc, In), for example the average Sc-O distance for the ScO_7-polyhedron in $ScMnO_3$ [34] is 2.40 Å and even larger as the one for the ScO_7-polyhedron in Sc_6ReO_{12} (2.21 Å). The average In(2)–O distance for the InO_7-polyhedron in $InMnO_3$ [35] is 2.27 Å and equal to the one for the InO_7-polyhedron in In_6ReO_{12}.

The ionic radii ratios $r(Re^{6+})/r(Sc^{3+})$ and $r(Re^{6+})/r(In^{3+})$ [4] are equal to 0.73 and 0.69, respectively, in agreement with the empirical criterion for the formation of the Ln_6MO_{12} phases with rhombohedral structure as proposed in [2] for the systems Ln_2O_3–MoO_3, Ln_2O_3–WO_3 and Ln_2O_3–UO_3.

3.4. Magnetic properties of In_6ReO_{12} and Sc_6ReO_{12}

The temperature dependence of inverse magnetization of Sc_6ReO_{12} is shown in Fig. 5. At low temperature a maximum of magnetization is observed at $T = 1.89(2)$ K (see inset). No significant difference between FC and ZFC data is detected. A magnetic moment of $0.65(1)\,\mu_B$ per Re-ion is calculated from the Curie constant in the paramagnetic region, obtained from fitting Eq. (4) to the

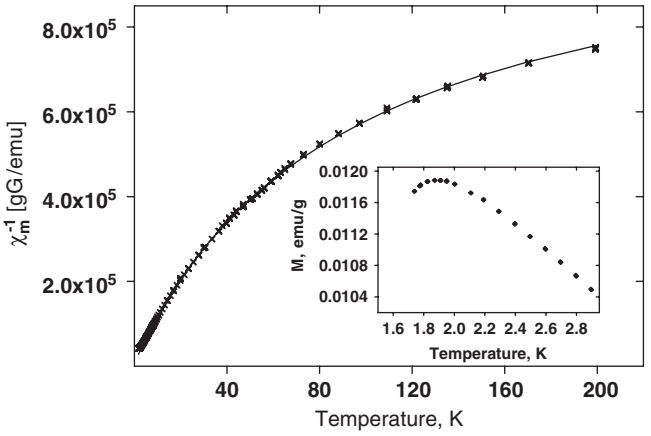

Fig. 5. Temperature dependence of magnetization (inset) and its inverse for Sc_6ReO_{12}.

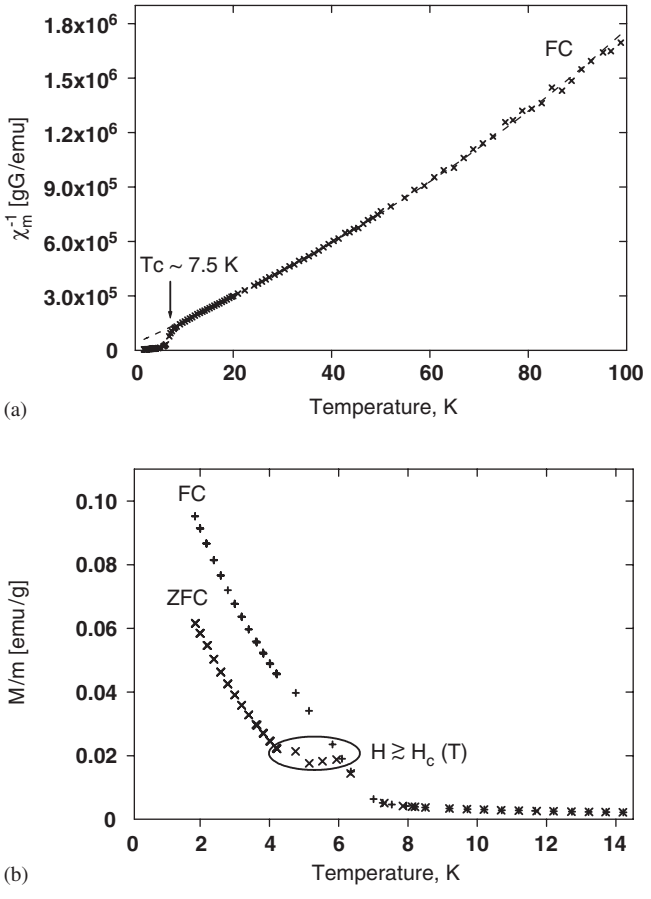

Fig. 6. (a) Temperature dependence of the inverse specific magnetic susceptibility of In_6ReO_{12}, measured in field-cooled (FC) mode. The dashed line represents a fit according to Eq. (4). (b) Comparison of magnetization data of In_6ReO_{12}, measured in field-cooled (FC) and zero-field cooled (ZFC) mode, respectively. In the marked region, the coercivity field becomes close to the applied field strength of 500 G, and the difference between FC and ZFC data is already considerably reduced below T_C.

Table 6
Magnetic properties of Sc_6ReO_{12} and In_6ReO_{12}

Compound	M_0 (emu/g)	Θ (K)	$\mu(Re^{+6})$ (μ_B)	Temperature range for fit, K
Sc_6ReO_{12}	$4.56(8)\times10^{-4}$	−0.7(1)	0.65(1)	10–200
In_6ReO_{12}	$-1.24(9)\times10^{-4}$	−3.2(3)	0.84(1)	15–100

The standard deviations in brackets are determined as the limits, for which an up to 10% higher residual is obtained in the least-square fit than for the optimum fit for Eq. (4).

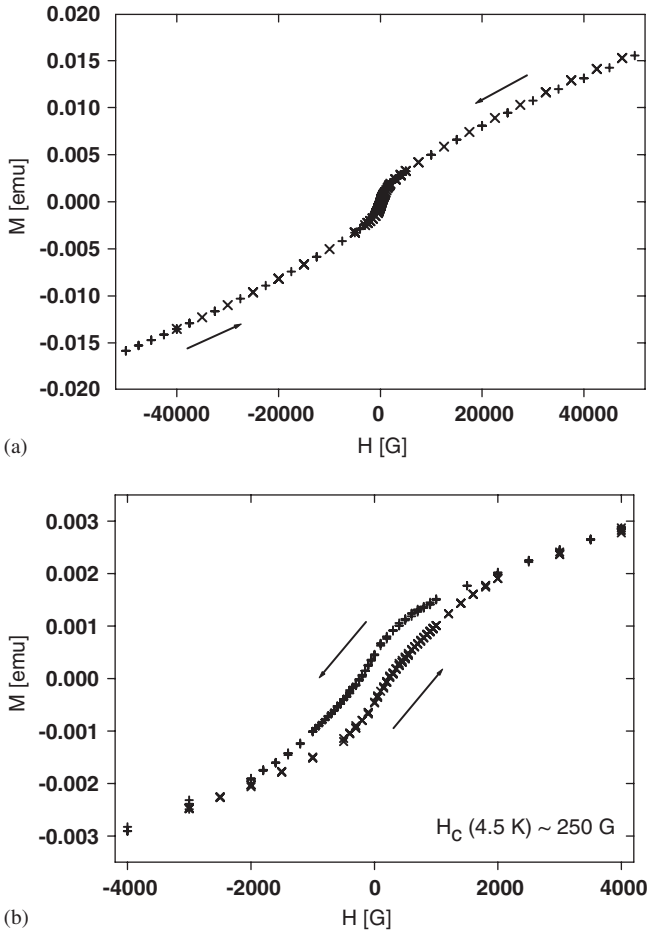

Fig. 7. (a) Hysteresis loop of In_6ReO_{12}, measured at 4.5 K. (b) Low-field section of the hysteresis loop of In_6ReO_{12}, measured at 4.5 K.

observed data.

$$M(T) = \frac{C}{T-\theta} + M_0. \quad (4)$$

This value is similar to those for other compounds with Re^{+6} ($5d^1$ electron configuration), for example 0.74 μ_B in Lu_6ReO_{12} [3] and 0.80 μ_B in $Sr_{11}Re_4O_{24}$ [36]. A maximum in the temperature dependence of magnetization was also observed for the isostructural compound Yb_6ReO_{12} at 2.15(10) K [3]. Additional neutron diffraction and magnetization studies at least down to 1.5 K are required to distinguish antiferromagnetic ordering from a spin-glass behaviour. The close values for the temperatures with maximum magnetization for Sc_6ReO_{12} and Yb_6ReO_{12} give evidence that the underlying effect is not dominated by the more and larger Yb^{3+} magnetic moments, but due to interactions within the Re^{+6}-sublattice.

In_6ReO_{12} reveals a pronounced increase of magnetization below $T_C = 7.5(5)$ K, shown as an abrupt decrease in the inverse specific susceptibility χ_m^{-1} in Fig. 6a. A magnetic moment of 0.84(1) μ_B per Re-ion is deduced from the paramagnetic region according to Eq. (4) with the parameters from Table 6. A ferromagnetic component is confirmed by the difference in magnetizations below T_C for data collection in FC and ZFC mode, see Fig. 6b. In the marked region between 4 and 6 K the zero-field cooled magnetization data approach successively those measured in field-cooled mode. This behaviour reflects the temperature dependence of the coercivity field $H_C(T)$, which becomes in this temperature region close to or lower than the applied field strength of 500 G. At 4.5 K the coercivity field is determined to about 250 G from the corresponding hysteresis loop, see Fig. 7(a) for the complete loop and Fig. 7(b) for the low-field region. The appearance of ferromagnetism in In_6ReO_{12} is rather surprising in the light of the more negative Curie–Weiss temperature θ than for Sc_6ReO_{12} and the nearest Re–Re distance of more than 6 Å. A possible mechanism might be based on an insulator to metal transition from Re^{+6} ions into Re^{+7} cores plus itinerant electrons. Note that a similar magnetic behaviour is also observed for $Sr_{11}Re_4O_{24}$ with Re^{+6} and Re^{+7} ions, which orders with a ferromagnetic component below the Curie temperature of $T_C = 12(1)$ K [36].

Acknowledgments

The authors are indebted to T. Kautz (Institut fuer Geowissenschaften, Johann Wolfgang Goethe Universitaet Frankfurt am Main, Germany) for help by performing the high-pressure high-temperature synthesis experiments. Financial support by the Deutsche Forschungsgemeinschaft (DFG FU125/42) is gratefully acknowledged.

References

[1] E.A. Aitken, S.F. Bartram, E.F. Juenke, Inorg. Chem. 3 (1964) 949–954.
[2] S.F. Bartram, Inorg. Chem. 5 (1966) 749–754.

[3] T. Hartmann, H. Ehrenberg, G. Miehe, G. Wltschek, H. Fuess, J. Solid State Chem. 148 (1999) 220–223.
[4] R.D. Shannon, Acta Crystallogr. A 32 (1976) 751–767.
[5] L. N. Komissarova. Inorganic and Analytical Chemistry of Scandium. Moscow, 2001, Editorial URSS (in Russian).
[6] V.A. Gagarina, V.V. Fomichev, L.Z. Gokhman, K.I. Petrov, Russ. J. Inorg. Chem. 22 (N7) (1977) 1832–1835 (Engl. Transl.).
[7] D. Michel, A. Kahn, Acta Crystallogr. B 38 (1982) 1437.
[8] A.P. Richard, D.D. Edwards, J. Solid State Chem. 177 (2004) 2740–2748.
[9] F.A. Cotton and G. Wilkinson, Advanced Inorganic Chemistry, fifth ed., Wiley, New York, 1988, 1455p.
[10] L.N. Komissarova, M.B. Varfolomeev, V.I. Ivanov, V.E. Plyutshev, Dokl. Akad. Nauk. 160 (3) (1965) 608–611 (in Russ).
[11] Ye. K. Kazenas, Vaporization Thermodynamics of Double Oxides, Nauka, Moscow, 2004, 551s (in Russian).
[12] V.N. Khrustalev, M.B. Varfolomeev, Yu.T. Struchkov, Russ. J. Inorg. Chem. 42 (1997) 1779–1784 (Engl. Transl.).
[13] V. Khrustalev, M. Varfolomeev, N. Shamrai, A. Vol'fkovich, Russ. J. Inorg. Chem. 43 (1998) 13 (Engl. Transl.).
[14] G.M. Sheldrick, Acta Crystallogr. A 46 (1990) 467–473.
[15] G.M. Sheldrick, SHELXL97, Program for the Refinement of Crystal Structures, University of Göttingen, Germany, 1997.
[16] Stoe & Cie, X-STEP32, Stoe & Cie GmbH. Darmstadt, Germany, 2000.
[17] CrysalisRed, CCD data reduction GUI, version 1.171.26, Oxford Diffraction Poland, 2005.
[18] T. Roisnel, J. Rodriguez-Carvajal, Mater. Sci. Forum 378–381 (2001) 118–123.
[19] H. Oppermann, Z. Anorg. Allg. Chem. 523 (1985) 135–144.
[20] K. Denbigh, The Principles of Chemical Eguilibrium. Cambridge, University Press, Cambridge, 1955, 491pp.
[21] V.A. Alyoshin, D.A. Mikhailova, E.V. Antipov, Physica C 271 (1996) 197–204.
[22] D.A. Mikhailova, V.A. Alyoshin, E.V. Antipov, J. Solid State Chem. 146 (1999) 151–156.
[23] H. Schäfer, Z. Anorg. Allg. Chem. 400 (1973) 253–284.
[24] G. Baud, J.-P. Besse, Mater. Res. Bull. 9 (1974) 1499.
[25] J.P. Besse, M. Bolte, G. Baud, R. Chevalier, Acta Crystallogr B 32 (1976) 3045.
[26] K.G. Bramnik, H. Ehrenberg, S. Buhre, H. Fuess, Acta Crystallogr. B 61 (2005) 246–249.
[27] T. Schleid, G. Meyer, J. Less-Common Met. 149 (1989) 73–80.
[28] V.A. Gagarina, V.V. Fomichev, O.I. Kondratov, K.I. Petrov, L.Z. Gokhman, E.M. Reznik, Russ. J. Inorg. Chem. 24 (1979) 1856–1863 (Engl. Transl.).
[29] M. Marezio, Acta Crystallogr B 48 (1992) 553–572.
[30] J. Zhang, R.B. von Dreele, L. Eyring, J. Solid State Chem. 104 (1993) 21–32.
[31] I.D. Brown, D. Altermatt, Acta Crystallogr. 20 (1966) 723–728.
[32] I.D. Brown, Acta Crystallogr B 48 (1992) 553–572.
[33] G.H. Rao, K. Bärner, I.D. Brown, J. Phys.: Condens. Matter 10 (48) (1998) L757–L763.
[34] M. Bieringer, J.E. Greedan, J. Solid State Chem. 143 (1999) 132–139.
[35] J.E. Greedan, M. Bieringer, J.F. Britten, D.M. Giaquinta, H.–C. Zur Loye, J. Solid State Chem. 130 (1995) 116–118.
[36] K.G. Bramnik, G. Miehe, H. Ehrenberg, H. Fuess, A.M. Abakumov, R.V. Shpanchenko, V. Yu. Pomjakushin, A.M. Balagurov, J. Solid State Chem. 149 (2000) 49–55.